EPA-600/R-95-161
November 1995

# SITE-SPECIFIC CHARACTERIZATION OF SOIL RADON POTENTIALS

Final Report

by

Kirk K. Nielson, Rodger B. Holt, and Vern C. Rogers
Rogers and Associates Engineering Corporation
O. O. Box 330, Salt Lake City, Utah 84110-0330

EPA Interagency Agreement RWFL933783
Florida DCA Contract 93RD-66-13-00-22-003
University of Florida Subcontract 1506481-12

DCA Project Officer: Mohammad Madani
Florida Department of Community Affairs
2740 Centerview Drive
Tallahassee, FL 32399

EPA Project Officer: David C. Sanchez
National Risk Management Research Laboratory
Research Triangle Park, NC 27711

University of Florida Project Director: Stanley Latimer
Department of Urban and Regional Planning
431 ARCH, University of Florida
Gainesville, FL 32611

Prepared for:
State of Florida
Florida Department of Community Affairs
2740 Centerview Drive
Tallahassee, FL 32399

and

U. S. Environmental Protection Agency
Office of Research and Development
Washington, DC 20460

**TECHNICAL REPORT DATA**
*(Please read Instructions on the reverse before comp*

PB96-140553

| | |
|---|---|
| 1. REPORT NO. EPA-600/R-95-161 | 2. |
| 4. TITLE AND SUBTITLE Site-Specific Characterization of Soil Radon Potentials | 5. REPORT DATE November 1995 |
| | 6. PERFORMING ORGANIZATION CODE |
| 7. AUTHOR(S) Kirk K. Nielson, Rodger B. Holt, and Vern C. Rogers | 8. PERFORMING ORGANIZATION REPORT NO. RAE-9226/1-12R1 |
| 9. PERFORMING ORGANIZATION NAME AND ADDRESS Rogers and Associates Engineering Corporation P. O. Box 330 Salt Lake City, Utah 84110 | 10. PROGRAM ELEMENT NO. |
| | 11. CONTRACT/GRANT NO. EPA Interagency Agreement RWFL933783 |
| 12. SPONSORING AGENCY NAME AND ADDRESS **EPA, Office of Research and Development** **Air Pollution Prevention and Control Division** **Research Triangle Park, NC 27711** | 13. TYPE OF REPORT AND PERIOD COVERED Final; 11/93 - 9/94 |
| | 14. SPONSORING AGENCY CODE **EPA/600/13** |

15. SUPPLEMENTARY NOTES APPCD project officer is David C. Sanchez, Mail Drop 54, 919/541-2979.

16. ABSTRACT The report presents a theoretical basis for measuring site-specific radon potentials. However, the empirical measurements suggest that the precision of such measurements is marginal, leaving an uncertainty of about a factor of 2 in site-specific estimates. Although this may be useful for some applications, it probably is inadequate for most decisions about construction of radon-resistant building features. Although more detailed site characterization (soil borings and measurements of radium, emanation, moisture, and permeability profiles) can improve precision, the additional expense may not be justified in comparison to the cost of more conservative use of radon-resistant building features. Field tests of soil radon flux and moisture measurements were conducted at 26 house sites in Polk County, Florida, to evaluate their utility in predicting site-specific radon potentials. Radon fluxes also were measured from bare concrete surfaces where they were accessible. Yard gamma-ray measurements were also conducted, but failed to show good correlation with the measured radon fluxes. The measured soil radon fluxes and moistures showed localized trends in radon potential that compared well with mapped radon potentials in some cases, but not in others. For the 26 houses, the site-specific radon potentials averaged twice the potentials from the generalized radon maps.

17. KEY WORDS AND DOCUMENT ANALYSIS

| a. DESCRIPTORS | b. IDENTIFIERS/OPEN ENDED TERMS | c. COSATI Field/Group |
|---|---|---|
| Pollution | Pouultion Control | 13B |
| Radon | Stationary Sources | 07B |
| Soils | | 08G, 08M |
| Measurement | | 14G |
| Residential Buildings | | 13M |

| | | |
|---|---|---|
| 18. DISTRIBUTION STATEMENT **Release to Public** | 19. SECURITY CLASS *(This Report)* Unclassified | 21. NO. OF PAGES 46 |
| | 20. SECURITY CLASS *(This page)* Unclassified | 22. PRICE |

EPA Form 2220-1 (9-73)

# FOREWORD

The U.S. Environmental Protection Agency is charged by Congress with protecting the Nation's land, air, and water resources. Under a mandate of national environmental laws, the Agency strives to formulate and implement actions leading to a compatible balance between human activities and the ability of natural systems to support and nurture life. To meet this mandate, EPA's research program is providing data and technical support for solving environmental problems today and building a science knowledge base necessary to manage our ecological resources wisely, understand how pollutants affect our health, and prevent or reduce environmental risks in the future.

The National Risk Management Research Laboratory is the Agency's center for investigation of technological and management approaches for reducing risks from threats to human health and the environment. The focus of the Laboratory's research program is on methods for the prevention and control of pollution to air, land, water, and subsurface resources; protection of water quality in public water systems; remediation of contaminated sites and groundwater; and prevention and control of indoor air pollution. The goal of this research effort is to catalyze development and implementation of innovative, cost-effective environmental technologies; develop scientific and engineering information needed by EPA to support regulatory and policy decisions; and provide technical support and information transfer to ensure effective implementation of environmental regulations and strategies.

This publication has been produced as part of the Laboratory's strategic long-term research plan. It is published and made available by EPA's Office of Research and Development to assist the user community and to link researchers with their clients.

E. Timothy Oppelt, Director
National Risk Management Research Laboratory

## EPA REVIEW NOTICE

This report has been peer and administratively reviewed by the U.S. Environmental Protection Agency, and approved for publication. Mention of trade names or commercial products does not constitute endorsement or recommendation for use.

This document is available to the public through the National Technical Information Service, Springfield, Virginia 22161.

## ABSTRACT

Radon gas generated from radium decay in soils can enter houses through foundation openings and accumulate to levels that pose significant risks of lung cancer with chronic exposure. The Florida Department of Community Affairs is developing construction standards to protect public health by requiring radon-resistant building features in areas of elevated soil radon potential. Although state-wide maps of soil radon potential have been developed to show the regions where the features are required, there is also a need for simple methods to assess the radon potential of specific building sites. Therefore, simple measurements to assess the radon potential of specific building sites are evaluated.

This report develops a mathematical basis for using simple site measurements to estimate soil radon potential. The approach utilizes a lumped-parameter model of radon generation and entry that was developed previously for Florida houses and soils from the more detailed RAETRAD numerical model. Site-specific soil radon potential is defined as the rate of radon entry into a reference house, consistent with the definition used previously for the radon potential maps. The models show that, in the simplest case, soil radon potential can be reduced to a simple function of two measurable parameters: the soil surface radon flux and the soil moisture (as a fraction of saturation). The flux gives the radon generation rate of the soil profile, and the moisture is a surrogate for radon transport parameters, including air permeability and radon diffusion coefficient. For comparison to indoor radon levels, the radon flux can also be related to sub-slab radon concentrations. Measurements of radon flux from concrete floor slabs also can be used to estimate the non-advective contribution to radon entry rates.

Field tests of soil radon flux and moisture measurements were conducted at 26 house sites in Polk County, Florida, to evaluate their utility in predicting site-specific radon potentials. Radon fluxes also were measured from bare concrete surfaces where they were accessible. Yard gamma-ray measurements also were conducted, but failed to show good correlation with the measured radon fluxes. The measured soil radon fluxes and moistures showed localized trends in radon potential that compared well with mapped radon potentials in some cases, but not in others. For the 26 houses, the site-specific radon potentials averaged two times the potentials from the generalized radon maps. A large geometric standard deviation (GSD=4.7) was associated with individual houses in this comparison.

Comparisons of the site-specific estimates with indoor radon levels at each site, using prior data on house leakage rates for seven houses, showed ratios (calculated/measured) that were generally low ($0.59 \pm 0.24$). Comparisons for all 26 houses, using the reference passive ventilation rate of 0.25 ach, produced ratios averaging $1.06 \pm 0.72$. Using concrete-surface radon flux measurements, in addition to the site radon potential measurements, gave an overall comparison ratio of $0.87 \pm 0.56$ for the 15 houses where they were measured, thus reducing the uncertainty of the comparison from the level otherwise associated with these houses.

This report presents a theoretical basis for measuring site-specific radon potentials. However, the empirical measurements suggest that the precision of such measurements is marginal, leaving an uncertainty of about a factor of two in site-specific estimates. Although this may be useful for some applications, it probably is inadequate for most decisions about construction of radon-resistant building features. Although more detailed site characterization (soil borings and measurements of radium, emanation, moisture, and permeability profiles) can give improved precision, the additional expense may not be justified in comparison to the cost of more conservative use of radon-resistant building features.

## TABLE OF CONTENTS


| Chapter | | | Page No. |
|---|---|---|---|
| | Abstract | | ii |
| | List of Figures | | v |
| | List of Tables | | vi |
| 1 | **INTRODUCTION** | | **1-1** |
| | 1.1 | Background and Objective | 1-1 |
| | 1.2 | Previous Estimates of Soil Radon Potentials | 1-2 |
| | 1.3 | Objective and Scope | 1-5 |
| 2 | **THEORETICAL BASIS AND PARAMETER SENSITIVITY** | | **2-1** |
| | 2.1 | The RAETRAD Model and the Reference House | 2-1 |
| | 2.2 | Lumped-Parameter Model | 2-4 |
| | 2.3 | Surrogate Estimates of Model Parameters | 2-6 |
| | 2.4 | Sensitivity Analyses | 2-9 |
| 3 | **FIELD TESTS** | | **3-1** |
| 4 | **TEST RESULTS AND ANALYSIS** | | **4-1** |
| | 4.1 | Empirical Correlations with Radon Flux | 4-1 |
| | 4.2 | Estimation of Site-Specific Soil Radon Potentials | 4-6 |
| | 4.3 | Comparison of Soil Radon Potentials with Indoor Radon Data | 4-9 |
| 5 | **DISCUSSION AND CONCLUSIONS** | | **5-1** |
| 6 | **LITERATURE REFERENCES** | | **6-1** |

## LIST OF FIGURES


| Figure No. | | Page No. |
|---|---|---|
| 1 | Two-dimensional grid and boundaries defining the house and soil regions analyzed by RAETRAD | 2-2 |
| 2 | Large-area sampler for measuring radon flux from concrete surfaces | 3-4 |
| 3 | Logarithmic regression of radon flux measurements on gamma-ray measurements for each site | 4-3 |
| 4 | Logarithmic regression of radon flux measurements on soil moisture for each site | 4-4 |
| 5 | Logarithmic regression of radon flux measurements on the surrogate flux parameter $J_{sur}$ for each site | 4-5 |
| 6 | Comparison of distributions of site-specific radon potentials calculated from measured data with radon potentials from the draft FRRP radon map | 4-8 |
| 7 | Comparisons of indoor radon estimated from site-specific measurements with measured concentrations using (a) generic slab diffusion properties or (b) measured radon fluxes from concrete slabs | 4-12 |

## LIST OF TABLES


| Table No. | | Page No. |
|---|---|---|
| 1 | Properties of the reference house used to estimate soil radon potentials | 2-3 |
| 2 | Reference values of soil parameters used in parametric fitting of radon entry velocities | 2-4 |
| 3 | FRRP data for the houses at the 26 study sites | 3-2 |
| 4 | Results of measurements at the 26 study sites | 4-2 |
| 5 | Comparison of site-specific and mapped soil radon potentials | 4-7 |
| 6 | Comparison of measured and calculated indoor radon concentrations | 4-10 |

# 1. INTRODUCTION

## 1.1 BACKGROUND AND OBJECTIVE

Radon ($^{222}Rn$) gas generated by naturally occurring radium ($^{226}Ra$) in soils can enter buildings through their foundations. With elevated entry rates and inadequate ventilation, it can accumulate indoors to levels that pose significant risks of lung cancer with chronic exposure. The U.S. Environmental Protection Agency (EPA) attributes 7,000 to 30,000 lung cancer fatalities annually to radon exposure, and recommends remedial action if indoor radon levels average four picocuries per liter (4 pCi $L^{-1}$) or higher (EPA92a,b). The EPA recommends reducing indoor radon levels below 4 pCi $L^{-1}$ where possible to approach outdoor ambient levels and further reduce health risks. Indoor radon levels average about 1.25 pCi $L^{-1}$ in the United States, and exceed 8 pCi $L^{-1}$ in about 1% of all U.S. homes (EPA92c).

Although outdoor air, building materials, and water supplies can also contribute to indoor radon, soil is usually the dominant source of elevated radon levels. The Florida Department of Community Affairs (DCA) and the EPA have jointly developed radon-resistant building standards to help reduce health risks by reducing radon entry from soils (San91). The standards address improved understructure sealing, altered air pressures, and other engineered features developed under the DCA's Florida Radon Research Program (FRRP). If integrated into state-wide building codes, the standards would add an incremental cost to new construction. This cost could be minimized by applying the standards only in areas of significant soil radon potential. State-wide radon potential maps are presently being developed to provide a basis for such targeted application of the standards (Nie95a). However, there is also a need for site-specific measurements of radon potential for local alternative decisions on applying the standards.

This report evaluates prototype methods for characterizing soil radon potentials at individual building sites. The methods would indicate more specifically the degree of radon resistance needed in constructing individual buildings. The methods could also be used to

make benchmark measurements for evaluating the more general, regional radon potential maps, which average over large spatial variations even within prescribed map regions.

## 1.2 PREVIOUS ESTIMATES OF SOIL RADON POTENTIALS

Soil radon potentials have been defined in previous studies from a variety of site-specific parameters, which have usually included localized indoor radon data, soil-gas radon concentrations, and soil air permeability. Other defining or correlating parameters have also included surface radon flux, soil radium concentration, moisture, density, porosity, gamma-ray activity, geologic classification, textural and lithologic properties, and water table or bedrock constraints.

Geographic classifications of land using indoor radon data, geology and lithology maps, geographic and physiographic groupings, and soil maps have been reviewed previously (Nie91). These classifications have been commonly applied to regional estimates rather than site-specific estimates. Indoor radon under these classifications was qualitatively defined from selected groupings or tiers of the regional or local parameters.

Several radon indices and simplified models have been proposed for estimating soil radon potential. One of the earliest (Eat84) was a Radon Index Number (RIN), which had the form:

$$RIN = h\,A / \log(k') \qquad (1)$$

where h = average ventilation period of the house
A = emanating radium concentration in the soil
k' = inverse of soil air permeability.

Another RIN was proposed (DSM85) to have the form:

$$RIN = \log(A) + 0.45 \log(k) \qquad (2)$$

where the 0.45 factor is a fitting constant based on numerical modeling of radon entry.

A later radon index was developed to interpret site-specific measurements of soil radon and air permeability. This RIN had the form (Kun89):

$$RIN = 10\ C\ \sqrt{k} \tag{3}$$

where 10 = factor to scale the index to basement radon concentrations
C = soil gas radon concentration (pCi $L^{-1}$)
k = soil gas permeability ($cm^2$).

Another radon index was called the radon availability number (RAN) (Tan89). It was defined as the amount of radon per unit area that can be delivered from soil to a building interface by diffusion and advection under an assumed pressure gradient. It was defined as:

$$RAN = 10^3\ C_{max}\ \varepsilon\ x \tag{4}$$

where $C_{max}$ = deep-soil radon concentration (pCi $L^{-1}$)
$\varepsilon$ = soil porosity
x = interstitial migration distance (m)

The RAN was related to the radon flux into a structure by multiplying by the foundation area of the structure and by the radon decay constant.

Two other radon indices were proposed to separate soil radon availability from house effects (Pea90). The first, the Geologic Radon Potential (GRP), was defined from an empirical three-tiered classification of two surrogate parameters: soil water permeability (inches $hour^{-1}$) and equivalent uranium (ppm). The second, the Integrated Radon Potential (IRP), would combine the GRP with house characteristics to estimate the percentage of homes expected to exceed 4 pCi $L^{-1}$ in radon screening measurements. The IRP was not specifically defined because of the inadequacy of data.

A more detailed approach for estimating soil radon potentials (Naz89) utilizes an analytical solution to the advective radon transport equation to predict indoor radon entry. Key parameters in this approach include soil air permeability, soil radon generation rate (radium concentration, density, and radon emanation coefficient), foundation crack geometry, and air suction parameters for the house. This approach represents more specifically the soil and house properties affecting radon entry, and overcomes the empirical parameter grouping and fitting that may describe particular data sets, but that fail in broader applications. This approach defines the radon potential as the rate of radon entry into the house (pCi $s^{-1}$).

A more detailed modeling approach for defining radon entry (Rog91c) also characterizes radon entry from detailed house and soil parameters, but includes radon diffusion in addition to advective radon transport. Based on the RAETRAD model (Nie94b), this approach utilizes detailed soil radium distributions; radon emanation fractions; and soil density, moisture, permeability, and diffusion coefficient in addition to house suction pressures and crack distributions. This approach defines soil radon potential on an annual basis (mCi $y^{-1}$) to emphasize the long-term average nature of equivalent steady-state radon entry rates and exposures.

A recent compilation of site-specific measurement methods (Yok92) emphasizes the need for detailed characterization of soil radon source and transport properties. The methods in this compilation are aimed at site-specific estimates of radon source potentials, and include numerous procedures for measuring soil density, particle size, texture classification, moisture, permeability, diffusion coefficient, radon emanation coefficient, radium concentration, and radon concentration profiles. While the study describes and compares many different measurement methods, its interpretation of each method's ability to predict soil radon potential or indoor radon levels is less quantitative. The measurement parameters are interpreted in terms of a radon source potential index, Y, which is defined as:

$$Y = 6{,}600\ EF_1\ EF_2\ EF_3\ C_{max} \sqrt{k\epsilon} \leq 0.07\ C_{max} \qquad (5)$$

where $EF_1$ = site drainage condition index

$EF_2$ = site groundwater condition index

$EF_3$ = wind, temperature, and aridity index

k = soil air permeability (>$6.5 \times 10^{-12}$ $m^2$).

The index is interpreted qualitatively as low radon source potential (Y≤0.5), moderate potential (0.5<Y≤1.5), high potential (1.5<Y≤7), and very high potential (Y>7). However, the study does not specify relations between these potentials and expected indoor radon levels.

For quantitative regional mapping of radon potentials in Florida, soil radon potentials have been defined (Nie95a) as the rate of radon entry into a hypothetical reference house, which is individually modeled on the soil profiles of each region being mapped. This approach eliminates house variations, and assesses local soil radon generation and transport properties for their effect on the same reference house. Although these calculations use detailed estimates of soil profiles, water distributions, radium and emanation properties, and other parameters, simplified models can allow use of the same approach for site-specific analyses, even if less detailed data are available. For modeling simplicity, the dominant features of the RAETRAD model have been reduced for Florida slab-on-grade houses to a simplified lumped-parameter model (Nie94a). This simplified model provides a potential basis for quantitative site-specific estimates of soil radon potential, which this report explores.

## 1.3 OBJECTIVE AND SCOPE

This report presents the theoretical basis and empirical tests of methods for evaluating the soil radon potential of specific sites. For consistency with existing soil radon potential maps, the soil radon potential is defined theoretically with the same reference house used for the maps. A lumped-parameter model (Nie94a) simplifies the theoretical basis, and indicates minimum parameters and surrogates for characterizing the site radon potential. Field tests of the methods included measurements of selected parameters and surrogates at a number of house sites that were already being studied by other contractors under the DCA's Florida Radon Research Program (FRRP). Soil radon potentials were estimated from the field measurements and were used to estimate indoor radon levels for comparison with measured

radon levels in the houses on the sites. The results were also compared with expected levels for the houses to evaluate the uncertainties associated with the radon potentials.

# 2. THEORETICAL BASIS AND PARAMETER SENSITIVITY

The site-specific soil radon potential is defined as the annual rate of radon entry from soils into a hypothetical reference house that is defined to represent Florida slab-on-grade houses. The reference house provides a constant, typical interface between the indoor exposure volume and the varied soil conditions that control radon potential. Although house and soil parameters cannot be completely separated for modeling radon entry, the use of a reference house avoids the large differences in radon potential that would otherwise result from differences in house design, construction, ventilation, and occupancy. The mathematical definition of site-specific radon potential utilizes a lumped-parameter model (Nie94a), which is based in turn on the detailed RAdon Emanation and TRAnsport into Dwellings (RAETRAD) model (Nie94b). For consistency with previous studies, the reference house and related model definitions are kept consistent with previous definitions used in radon potential mapping (Nie95a) and radon entry modeling (Nie94a,b).

## 2.1 THE RAETRAD MODEL AND THE REFERENCE HOUSE

The detailed RAETRAD model provides the primary basis for defining soil radon potentials. RAETRAD simulates radon production in soils, slabs, and footings, and simulates radon movement and entry through the pores and openings of the soil-house interface by both diffusion (concentration-driven) and advection (with pressure-driven air flow). RAETRAD utilizes the complete multi-phase theory of radon generation, decay, transport, absorption, and adsorption (Rog91a, Rog93) to characterize radon entry using a two-dimensional numerical-analytical algorithm (Nie94b). The algorithm solves LaPlace's equation to define steady state air pressure distributions under and near the house and to obtain air flow velocities, which are used in subsequent radon calculations. The radon differential equation also is solved in steady state, and incorporates the air velocity field to compute simultaneous diffusive and advective radon transport. The equations are solved numerically in elliptical-cylindrical geometry to represent houses of different size and with varying rectangular aspect (length/width) ratios.

RAETRAD computes radon entry rates into a house by integrating the total radon transport across the floor surface area. Indoor radon concentrations also are estimated from the computed entry rates by dividing them by the house volume and air ventilation rate. Figure 1 illustrates the geometry of the reference house and the surrounding soil regions analyzed by RAETRAD.

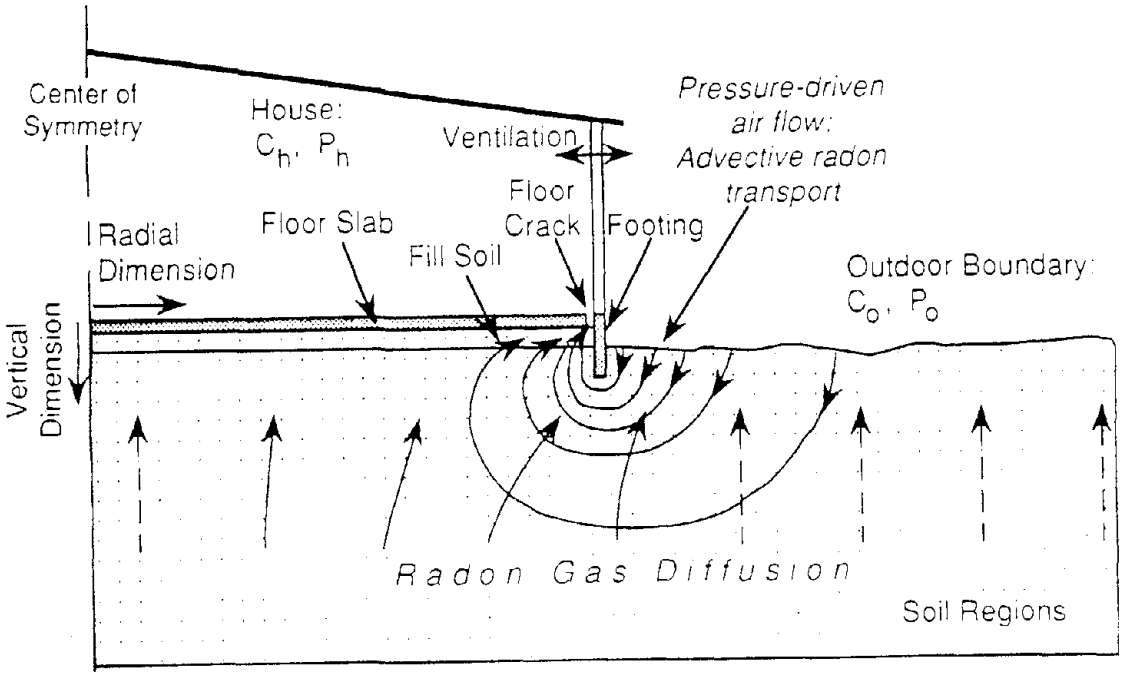


**Figure 1. Two-dimensional grid and boundaries defining the house and soil regions analyzed by RAETRAD.**

The reference house analyzed by RAETRAD is defined to correspond to the reference house used previously for radon potential mapping. Its fundamental properties are listed in Table 1. As represented schematically in Figure 1, the house is a slab-on-grade single-family dwelling measuring 8.6 x 16.5 m (28 ft. x 54 ft.). Its volume is based on that of a median U.S. family dwelling (Naz88), and is similar to that of typical Florida houses (Acr90). Its area is estimated from its volume using a nominal 2.4-m

(8-ft) ceiling height, and is similar to other estimates of Florida floor slab areas (Acr90). Its ventilation rate is about half the normal median U.S. house ventilation rate (Naz88), based on measurements in Florida houses (Cum92). A perimeter floor crack approximates a floating-slab shrinkage crack to permit advective radon entry from pressure-driven air flow. The stem wall and footing penetrate 61 cm (2 ft) into the natural terrain, and enclose an additional 30 cm (1 ft) of above-grade fill soil beneath the slab. The indoor pressure is typical of that resulting from thermal and wind-induced indoor pressures in U.S. homes (Naz87), and also of the average indoor pressures measured in a group of 70 Florida houses (Cum92) under passive conditions. Concrete slab air permeabilities, radon diffusion coefficients, and other properties are estimated from data measured on Florida floor slabs (Rog94).

**Table 1. Properties of the reference house used to estimate soil radon potentials.**

| | | | |
|---|---|---|---|
| House Area | 143 $m^2$ | Crack Permeability | $4x10^{-5}$ $cm^2$ |
| House Dimensions | 8.6 x 16.5 m | Indoor Pressure | -2.4 Pa |
| House Length/Width | 1.9 (ratio) | Concrete Slab Thickness | 10 cm |
| House Volume | 350 $m^3$ | Concrete Slab Porosity | 0.22 |
| House Ventilation Rate | 0.25 $h^{-1}$ | Concrete Slab $^{226}Ra \cdot$ Emanation | 0.07 pCi $g^{-1}$ |
| Floor Crack Width | 0.5 cm | Exterior Footing Depth | 61 cm |
| Floor Crack Location | slab perimeter | Concrete Air Permeability | $1x10^{-11}$ $cm^2$ |
| Crack Area Fraction | 0.002 | Concrete Rn Diffusion Coeff. | $8x10^{-4}$ $cm^2$ $s^{-1}$ |

Soils beneath the reference house are modeled as uniform, isotropic soils having the properties listed in Table 2. A 30-cm layer of sandy fill soil is located beneath the slab, below which the site-specific soil is represented by its approximate textural class and its associated water content at a matric potential of -30 kPa (Nie92). From these properties, the soil air permeability and radon diffusion coefficient are calculated from empirical relationships (Rog91b).

**Table 2. Reference values of soil parameters used in parametric fitting of radon entry velocities**

| | | | |
|---|---|---|---|
| Fill soil | sand (30 cm) | Fill moisture (sat'n fraction) | 0.213 |
| Water matric potential | -30 kPa | Sand moisture (sat'n fraction) | 0.100 |
| Density | 1.6 g $cm^{-3}$ | Sandy loam moisture (sat'n fraction) | 0.461 |
| Porosity | 0.407 | Loam moisture (sat'n fraction) | 0.646 |
| Radium concentration | variable | Clay loam moisture (sat'n fraction) | 0.712 |
| Radon emanation | variable | Clay moisture (sat'n fraction) | 0.832 |

## 2.2 LUMPED-PARAMETER MODEL

The lumped-parameter model was developed primarily from RAETRAD sensitivity analyses, which identified the most significant house and soil parameters. The analyses suggested simplified approximations to express average indoor radon levels as a function of radon source strength and house radon resistance and ventilation parameters. The radon source strength was defined in terms of the sub-slab radon concentration. The house radon resistance was defined from floor openings, pressure driving forces, and slab diffusivity (Nie94a).

The lumped-parameter model uses the following relation between indoor radon and the radon entry rate (Nie94a):

$$C_{net} = C_{in} - C_{out} = 3.6\ Q / (\lambda_h\ V_h) \qquad (6)$$

where $C_{net}$ = net indoor radon concentration from sub-slab sources (pCi $L^{-1}$)

$C_{in}$ = total indoor radon concentration (pCi $L^{-1}$)

$C_{out}$ = outdoor background radon concentration (pCi $L^{-1}$)

3.6 = unit conversion (pCi $L^{-1}$ $h^{-1}$ per pCi $m^{-3}$ $s^{-1}$)

Q = radon entry rate (pCi $s^{-1}$)

$\lambda_h$ = rate of house ventilation by outdoor air ($h^{-1}$)

$V_h$ = h $A_h$ = interior house volume ($m^3$)

h = mean height of the interior volume of the house (m)

$A_h$ = house area ($m^2$).

The radon entry rate in equation (6) is defined in the lumped-parameter model for the reference house as:

$$Q = A_h C_{sub} [f_c (v_{dc} - v_{ac}\Delta P) + v_{slab} + v_{sc}] \quad (7)$$

where $C_{sub}$ = sub-slab radon concentration (pCi $L^{-1}$)

$f_c$ = area of floor openings as a fraction of total floor area (dimensionless)

$v_{dc}$ = equivalent velocity of radon diffusion through floor openings, dependent on the radon diffusion coefficient of the soil (0.0143 mm $s^{-1}$)

$v_{ac}$ = equivalent velocity of radon advection through floor openings, dependent on the air permeability of the soil (mm $s^{-1}$ $Pa^{-1}$) = $\exp(-3\text{-}0.045e^{6S})$

S = soil water saturation fraction (dimensionless)

$\Delta P$ = indoor air pressure (Pa)

$v_{slab}$ = equivalent velocity of radon diffusion through the floor slab, dependent on the radon diffusion coefficient of the slab concrete (mm $s^{-1}$) = $2.9\text{x}10^{-7} \exp(11.4W)$

W = water/cement ratio of the slab concrete (dimensionless)

$v_{sc}$ = radon entry velocity adjustment for house size and crack location (mm $s^{-1}$) = $3.5\text{x}10^{-5}(x_{crk}/x_h) + 4.6\text{x}10^{-5}/x_h$

$x_{crk}$ = location of dominant floor crack opening from house perimeter (m)

$x_h$ = house width (m).

Only the parameters $C_{sub}$ and $v_{ac}$ in equation (7) are site-dependent; therefore reference-house values were substituted for all of the others, leading to the following relationship for defining the site-specific soil radon potential:

$$Q_{ss} = 1.68\, C_{sub} [0.019 + \exp(-3 - 0.045\, e^{6S})] \quad (8)$$

where $Q_{ss}$ = site-specific soil radon potential (pCi $s^{-1}$).

Although the indoor radon concentration for a reference house can be directly estimated by using $Q_{ss}$ in equation (6), indoor radon concentrations for specific houses are better estimated by directly using as many defining parameters as are known in the lumped-parameter model. Using the definitions associated with equation (7) to define the radon entry rate (Q) for use in equation (6), the indoor radon concentrations can be estimated using house-specific data.

## 2.3 SURROGATE ESTIMATES OF MODEL PARAMETERS

Many of the model parameters are difficult to measure directly, and therefore are seldom quantified. However, most can be estimated from related parameters that are directly measurable. The site-specific value for the soil water saturation fraction (S) can be readily estimated from measured values of the soil moisture content as:

$$S = 0.01\, M_v/\varepsilon = 0.01\, \rho M_w/\varepsilon \qquad (9)$$

where $M_v$ = soil moisture (volume percent)

$\varepsilon$ = total soil porosity (dimensionless) = $1 - \rho/\rho_g$

$\rho$ = soil bulk dry density (g $cm^{-3}$)

$\rho_g$ = soil specific gravity (nominally 2.7 g $cm^{-3}$)

$M_w$ = soil moisture (dry weight percent).

Site-specific values for $C_{sub}$ should utilize sub-slab radon concentration measurements if they are available. Measurements should be made just beneath the vapor barrier membrane at the slab-soil interface. However, in more common situations where such data are unavailable, $C_{sub}$ can also be estimated from other, surrogate measurements. The best surrogate for $C_{sub}$ is a measurement of radon flux on a soil profile corresponding to the soil profile under the slab. If the soil is homogeneous and isotropic, $C_{sub}$ can be estimated from the surface radon flux measurement, the radon source and diffusion properties of the concrete

(c subscripts), and the radon diffusion coefficient and depth of the radon-generating soil profile (s subscripts) as:

$$C_{sub} = 10^3 \frac{R_c\rho_c E_c [\cosh(\alpha_c x_c) - 1] + 10^{-4} J_s \sinh(\alpha_c x_c) / \sqrt{\lambda D_c}}{p'_c \cosh(\alpha_c x_c) + p'_s \sinh(\alpha_c x_c) \tanh(\alpha_s x_s) \sqrt{D_s/D_c}} \quad (10)$$

where $R_i$ = soil or concrete $^{226}Ra$ concentration (pCi $g^{-1}$)

$i$ = s for soil or c for concrete

$\rho_i$ = soil or concrete density (g $cm^{-3}$)

$E_i$ = soil or concrete radon emanation coefficient (dimensionless)

$\alpha_i$ = $\sqrt{\lambda/D_i}$

$x_i$ = soil or concrete thickness (cm)

$J_s$ = radon flux at the soil surface (pCi $m^{-2}$ $s^{-1}$)

$D_i$ = radon diffusion coefficient of the soil or concrete pore space ($cm^2$ $s^{-1}$)

$p'_i$ = $p_i (1 - m_i + k'm_i)$

$p_i$ = soil or concrete porosity (dimensionless)

$m_i$ = soil or concrete moisture saturation fraction (dimensionless)

$k'$ = 0.26 pCi $cm^{-3}$ water per pCi $cm^{-3}$ air (from Henry's Law)

cosh = hyperbolic cosine function

sinh = hyperbolic sine function.

tanh = hyperbolic tangent function

Using the reference-house slab parameters from Table 1, and assuming the radon-generating soil profile is deep (unconstrained by a shallow water table or bedrock), $C_{sub}$ can be approximated from equation (10) as:

$$C_{sub} = (90 + 5{,}900\ J_s) / (1.13 + 35 \sqrt{D_s}) \quad (11)$$

The sub-slab radon concentration also can be estimated from soil-gas radon measurements, instead of from surface radon flux measurements. For cases where radon production by the concrete slab is negligible and the sub-slab soil and water profiles are uniform, the sub-slab radon concentration can be estimated from the relationship:

$$C_{sub} = C_s / \{1 + \coth(\alpha_c x_c) [1 - \cosh[\alpha_s(x_s - x)]/\cosh(\alpha_s x_s)]\} \quad (12)$$

where $C_s$ = soil radon concentration at depth x (pCi $L^{-1}$)
coth = hyperbolic cotangent function
x = depth of soil radon sample (cm).

For other cases, in which significant radon is produced by the slab, or where the soil exhibits significantly layered radium or moisture distributions, the sub-slab radon concentration can be determined from soil radon measurements using a multi-layered computer code such as the RAECOM code (Rog84a). Using the reference-house slab diffusion properties, equation (12) simplifies to:

$$C_{sub} = C_s / \{1 + 2.14 [1 - \cosh[\alpha_s(x_s - x)]/\cosh(\alpha_s x_s)]\}. \quad (13)$$

If the radon flux from the surface of the concrete slab is measured in addition to either the sub-slab concentration or a surrogate (soil radon flux or soil radon concentration), the diffusion coefficient of the slab, $D_c$, can be estimated for use in subsequent comparisons of the measured and predicted indoor radon concentrations. The value of $D_c$ cannot be solved explicitly, but it can be determined iteratively from the relation:

$$J_c = \{J_s + 10^4 R_c \rho_c E_c \sqrt{\lambda D_c}[\sinh(\alpha_c x_c) + Y[\cosh(\alpha_c x_c) - 1]]\} / \{\cosh(\alpha_c x_c) + Y \sinh(\alpha_c x_c)\} \quad (14)$$

where $Y = (p_s/p_c) \sqrt{D_s/D_c} \tanh(\alpha_s x_s)$.

Similar calculations for layered soil conditions can also utilize the RAECOM code (Rog84a).

For cases where soil radium concentrations and radon emanation coefficients are known, the following form of equation (10) may be used to estimate $C_{sub}$ from these more specific data in place of the surface radon flux:

$$C_{sub} = 10^3 \frac{R_c\rho_c E_c [\cosh(\alpha_c x_c) - 1]/p_c' + R_s\rho_s E_s Y \sinh(\alpha_c x_c)/p_s'}{\cosh(\alpha_c x_c) + Y \sinh(\alpha_c x_c)} \quad (15)$$

The ventilation rate in equation (6) can be defined as:

$$\lambda_h = a|\Delta P|^n + b \quad (16)$$

where a = rate of air infiltration at 1 Pa pressure differential ($h^{-1}$)

n = pressure exponent from blower-door test (dimensionless)

b = rate of air infiltration under passive conditions ($h^{-1}$).

If the *b* term in equation (16) is zero, the equation corresponds directly to the relationship determined by standard blower-door testing of the leakage area of a house (AST87). The *b* term is included in the lumped-parameter model to account for small, age-related increases in building leakage (Nie94a), but is also a convenient fitting parameter to avoid zero values for $\lambda_h$ under passive conditions when $\Delta P \approx 0$. Physically, the *b* term corresponds to the leakage due to random, turbulent fluctuations around $\Delta P = 0$, which may have a magnitude of the order of $\pm$2-3 Pa (Hin93).

## 2.4 SENSITIVITY ANALYSES

Several sensitivity analyses have been performed on the lumped-parameter model (Nie94a, Nie95b). These have demonstrated the relatively strong dependence of soil radon potentials on $C_{sub}$, $\lambda_h$, W, $\Delta P$, S, h, and $f_c$, and a smaller dependence on $v_{dc}$, $x_h$, $x_{crk}$. Field measurements therefore were

investigated for primarily identifying appropriate values of the important parameters. In cases where the values could not be adequately measured, default values found to be typical for the reference house were used.

# 3. FIELD TESTS

A series of site-specific field measurements was conducted on March 17-22, 1993 to evaluate the sensitivity, precision, and utility of selected field measurements for estimating site-specific radon potential. The measurements were conducted in the yards of 26 houses in Polk County, Florida, accompanying FRRP indoor radon measurements made by Southern Research Institute (SRI) in each of the houses. Each set of measurements was conducted within the building lot of an existing house for which indoor radon data also were available. This approach permitted comparison of the site-specific radon potential estimates with the measured indoor radon levels for each site. Table 3 describes the physical properties of each house and lists the house indoor radon levels as measured previously in the FRRP. As indicated by Table 3, data for several of the parameters were unavailable for many of the houses.

The field protocol at each site involved measurements on each of the four sides of the house of soil moisture, gamma-ray activity, and radon flux. In addition, a single measurement of radon flux was made on a bare concrete surface where such locations were accessible. The site measurement protocol concentrated mainly on measurements that could be made rapidly, with minimum expense, and that would most directly estimate the site-specific radon potential, $Q_{ss}$. As indicated by equation (8), the sub-slab radon concentration ($C_{sub}$) and the soil water saturation fraction (S) were of primary interest. To estimate S, soil moisture was measured using a time-domain Instrument for Reflectometric Analysis of Moisture in Soil (IRAMS, CPN Corporation, Martinez, CA). The instrument provided a volumetric moisture percentage in the top 30 cm of soil using a 30-cm wave-guide probe that could be inserted at any location for in-situ moisture measurements. Measurements with this instrument were used to estimate S with equation (9), assuming a generic soil porosity of $\varepsilon$=0.407 (see Table 2).

**Table 3. FRRP data for the houses at the 26 study sites**

| RAE No. | FRRP No. | Age[a] (yr) | Nbhd.[b] | SSV[c] system | Found.[d] | $\lambda_h$[e] Passive (ach) | Height[f] (ft) | Area[g] ($ft^2$) | Indoor Radon[h] (pCi $L^{-1}$) | Subslab Radon (pCi $L^{-1}$) |
|---|---|---|---|---|---|---|---|---|---|---|
| 1 | E-34 | 0 | A | None | SSW | --- | 9 | 1,024 | 2.1 ± 0.1 | --- |
| 2 | E-36 | 0 | A | None | SSW | --- | 9 | 1,781 | 1.9 ± 0.4 | --- |
| 3 | E-30 | 0 | A | None | SSW | --- | 12 | 2,733 | 2.7 ± 0.8 | --- |
| 4 | E-31 | 0 | A | None | SSW | --- | 16 | 2,450 | 1.6 ± 0.4 | --- |
| 5 | E-42 | 2 | B | None | SSW | --- | 18 | 2,216 | 2.1 ± 0.1 | --- |
| 6 | E-38 | 2 | B | None | SSW | --- | 10 | 2,835 | 2.2 ± 0.8 | --- |
| 7 | E-35 | 2 | --- | None | SSW | --- | 8 | 2,994 | 5.8 ± 2.0 | --- |
| 8 | E-40 | 1 | C | None | SSW | --- | 18 | 2,145 | 4.4 ± 0.6 | --- |
| 9 | E-41 | 2 | C | None | SSW | --- | 8 | 2,070 | 5.0 ± 1.3 | --- |
| 10 | E-37 | 1 | D | None | SSW | --- | 8 | 1,863 | 1.9 ± 0.4 | --- |
| 11 | E-22 | 1 | D | Passive | SSW | 0.27 | 8.3 | 2,270 | 3.0 ± 0.4 | 2,680 |
| 12 | E-32 | 1 | D | --- | SSW | --- | 8 | 1,968 | 2.3 ± 0.0 | --- |
| 13 | B-08 | 21 | --- | Active | SSW | --- | 8 | 2,584 | 37.5 | 24,000 |
| 14 | E-13 | 1 | --- | Active | Mono. | 0.50 | 10 | 2,715 | 1.7 | --- |
| 15 | E-24 | 1 | E | Passive | Mono. | 0.37 | 11 | 2,456 | 2.0 | 2,820 |
| 16 | E-45 | 1 | E | --- | Mono. | --- | 9 | 2,514 | 4.0 ± 1.7 | --- |
| 17 | E-11 | 1 | E | Passive | Mono. | 0.46 | 10 | 2,715 | 1.6 ± 1.1 | --- |
| 18 | D-08 | 18 | F | --- | Mono. | --- | 8 | 1,900 | 6.2 ± 2.2 | --- |
| 19 | D-06 | 18 | F | --- | Mono. | --- | 8 | 1,296 | 3.0 ± 0.5 | --- |
| 20 | C-14 | 18 | F | --- | Mono. | --- | 8 | 1,519 | 6.0 ± 1.6 | --- |
| 21 | D-11 | 18 | F | --- | Mono. | --- | 8 | 2,100 | 14.8 ±3.6 | --- |
| 22 | D-10 | 18 | F | --- | Mono. | --- | 8 | 1,980 | 5.7 ± 1.5 | --- |
| 23 | E-25 | 0 | G | Passive | Mono. | 0.25 | 10 | 1,876 | 2.4 ± 0.6 | 4,510 |
| 24 | E-39 | 0 | G | None | Mono. | --- | 9 | 1,692 | 3.2 ± 1.1 | --- |
| 25 | E-16 | 0 | G | Active | Mono. | 0.44 | 10 | 1,876 | 2.5 ± 0.8 | 4,080 |
| 26 | E-12 | 0 | G | Passive | Mono. | 0.48 | 10 | 2,715 | 2.5 ± 1.1 | --- |

[a]Rounded to the nearest whole year.

[b]Houses within approximately 100 m of each other are grouped by neighborhood.

[c]Sub-slab ventilation system: passive systems were capped; active systems were operational in E-13 and E-16 only.

[d]Foundation observations: slab in stem wall (SSW) assumed for concrete block stem walls; monolithic slab & stem wall (Mono.) assumed for poured stem walls. Some unobserved cases assumed identical to neighboring houses of same age.

[e]Air changes per hour, extrapolated to 2.4 Pa from blower-door data at higher pressures.

[f]Heights exceeding 12 ft are two-story structures.

[g]Area of living space, excluding garage.

[h]3-month alpha track measurement or mean ± standard deviation for two quarters.

Although prior FRRP measurements of $C_{sub}$ were planned for primary evaluations, these data were generally unavailable, and consisted of only single measurements in some reported cases. Therefore, the soil surface radon flux measurements were made at each site as the primary estimator of $C_{sub}$, using equation (11) as the basis for the calculation. The flux measurements were made using the small-canister method (Nie93), which has been shown previously to give equivalent results (Rog84b) to EPA Method 115 (EPA89). The radon fluxes were sampled over a 24-hour period, after which the charcoal canisters were retrieved, sealed, and submitted for laboratory assay of radon activity. The value of $D_s$ required for calculating $C_{sub}$ was estimated from the same porosity and moisture value using the predictive correlation (Rog91b):

$$D_s = D_o \varepsilon \exp(-6\varepsilon S - 6S^{14\varepsilon}) \qquad (17)$$

where $D_o$ = diffusion coefficient for radon in air (0.11 $cm^2\ s^{-1}$).

The additional radon flux measurements on bare concrete slab surfaces, when accessible, more directly estimated the radon moving through the concrete slabs. These flux measurements can potentially be used in equation (14) to estimate concrete slab diffusivity, and also provide an estimate of radon entry through the intact portions of the slabs. The flux measurements can be used more directly, however, to estimate $v_{slab}$ for use in equation (7) as:

$$v_{slab} = J_{slab}/C_{sub} \qquad (18)$$

where $J_{slab}$ = radon flux from the concrete slab surface (pCi $m^{-2}\ s^{-1}$).

The small-canister protocol (Nie93) was found to have marginal sensitivity for the low fluxes coming from concrete surfaces. Therefore, an alternative method was used, as illustrated in Figure 2. In this method, approximately 230 $cm^3$ of granular activated carbon (10 mesh, Marine Enterprises, Towson, MD) was spread over a paper napkin mounted in a 30-cm diameter wooden compression frame and covered with a polyethylene sheet. The frame

was sealed to the concrete surface with rope caulk (0.16 cm diameter, Frost King, Thermwell Products, Los Angeles, CA). The sampler was deployed for approximately 24 hours, after which the charcoal was retrieved and sealed into metal cans for gamma-ray assay of radon in a laboratory. The method was calibrated against the small-canister samplers using a thin-sample radon source at Rogers & Associates Engineering Corporation (Salt Lake City). The alternative method measured fluxes equal to those measured by the small-canister method, but provided a sensitivity improvement of a factor of 13.

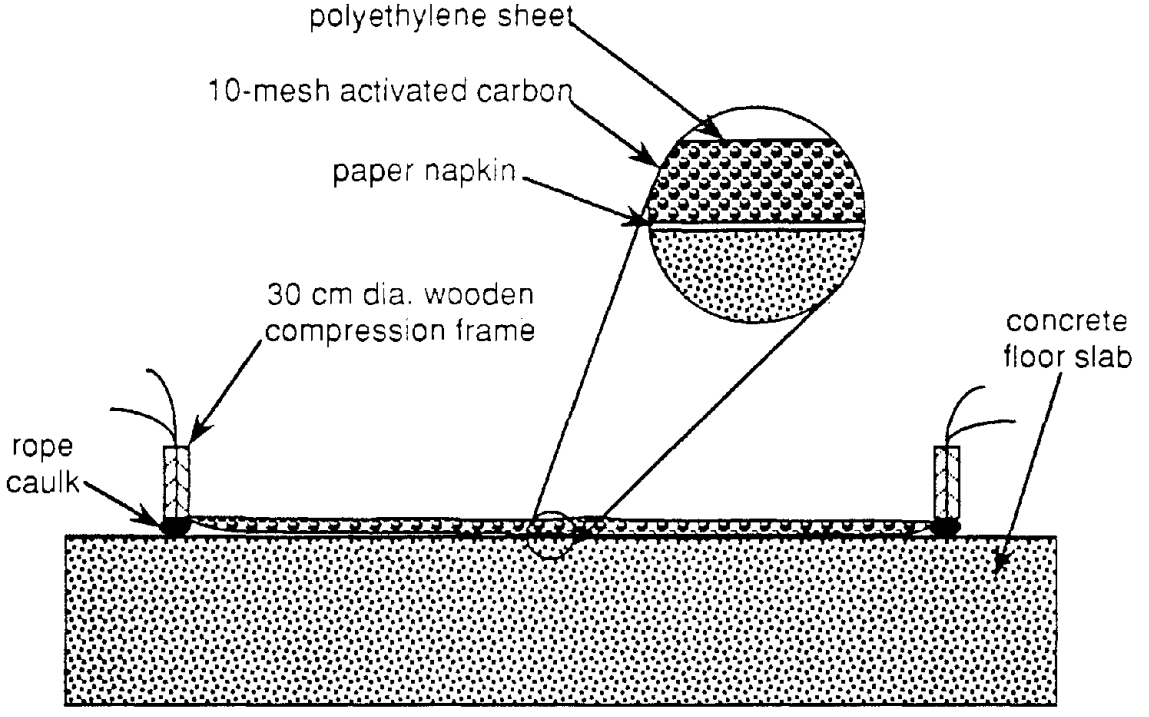


**Figure 2. Large-area sampler for measuring radon flux from concrete surfaces.**

The gamma-ray exposure measurements at the site were measured for possible correlation with the soil radon flux measurements, or as potential surrogates for surface soil radium concentration. The measurements were made at 1 m above the soil surface using a 5 x 5-cm sodium iodide scintillation probe and scaler (Models 44-23 and 2220, Ludlum Measurements Inc., Sweetwater, TX). The count rates were in turn calibrated against a tissue-equivalent meter (Model 1010, Radiation Measurement Systems) to convert the counts to $\mu R\ h^{-1}$ units (690 counts $min^{-1}$ per $\mu R\ h^{-1}$).

# 4. TEST RESULTS AND ANALYSIS

The site-specific measurements were analyzed for simple empirical correlations between the measured soil radon fluxes. They also were used to predict site-specific radon potentials, which in turn were compared with the FRRP indoor radon concentration data.

## 4.1 EMPIRICAL CORRELATIONS WITH RADON FLUX

The results of the site-specific measurements are presented in Table 4, summarized as means and standard deviations of the four replicate measurements for the gamma, moisture, and soil radon flux data. The data for each parameter were initially examined to assess the significance of differences between the different house sites. As suggested by comparison of the standard deviations of the means with the averages of the site standard deviations (at the bottom of Table 4), the gamma measurements show highly significant differences among the different house sites. The soil radon flux measurements show smaller, but still significant differences among the different house sites, and the moisture measurements show much smaller differences among the different sites. All of the differences were significant at the $p<0.01$ level in analyses of variance.

The potential correlation between soil radon flux measurements and yard gamma measurements next was examined by least-squares linear regression. Since radon flux varies directly as radium concentration for uniform soils, a linear relationship is expected. The regression on gamma intensity ($\gamma$ in $\mu R\ h^{-1}$) exhibited a correlation coefficient of only $r=0.26$ for the fitted line $J_s = -0.2 + 0.146\ \gamma$. Corresponding regressions of the site-averaged values, as reported in Table 4, yielded a slightly higher correlation coefficient of $r=0.36$ for the fitted line $J_s = -0.3 + 0.150\ \gamma$. Since the data are arguably distributed log-normally, a linear regression also was examined for the logarithms of the data, as illustrated by the plot in Figure 3. The fitted line, corresponding to $J_s = 0.23\ \gamma^{0.62}$, is strongly affected by numerous low flux points that occur at high gamma intensities. The low fluxes may result from high water tables or soil irrigation. In any event, the large scatter in the flux-gamma relationship limits the potential uses of gamma intensities as a surrogate for estimating soil radon flux.

**Table 4. Results of measurements at the 26 study sites**

| RAE No. | FRRP No. | Yard Gamma[a] ($\mu R\ h^{-1}$) | Soil Moisture[a] (vol. %) | Soil Radon Flux[a] ($pCi\ m^{-2}\ s^{-1}$) | Slab Radon Flux[b] ($pCi\ m^{-2}\ s^{-1}$) |
|---|---|---|---|---|---|
| 1 | E-34 | 21.9 ± 3.9 | 22.0 ± 4.5 | 0.61 ± 0.93 | 0.142 ± 0.003 |
| 2 | E-36 | 20.5 ± 3.4 | 19.2 ± 2.2 | 0.36 ± 0.17 | 0.193 ± 0.003 |
| 3 | E-30 | 32.1 ± 4.5 | 19.1 ± 10.7 | 0.50 ± 0.35 | 0.185 ± 0.003 |
| 4 | E-31 | 30.0 ± 6.9 | 22.4 ± 6.4 | 0.38 ± 0.11 | 0.168 ± 0.003 |
| 5 | E-42 | 37.2 ± 1.8 | 19.9 ± 2.1 | 0.76 ± 0.17 | 0.066 ± 0.003 |
| 6 | E-38 | 23.2 ± 4.7 | 20.4 ± 3.8 | 0.35 ± 0.11 | 0.023 ± 0.003 |
| 7 | E-35 | 16.3 ± 4.6 | 25.6 | 1.02 ± 1.34 | 0.108 ± 0.003 |
| 8 | E-40 | 8.7 ± 1.4 | 14.0 | 3.74 ± 3.87 | 0.208 ± 0.003 |
| 9 | E-41 | 8.5 ± 1.2 | 14.0 | 3.76 ± 3.47 | 0.302 ± 0.004 |
| 10 | E-37 | 6.6 ± 1.4 | 12.0 | 0.38 ± 0.13 | ---[c] |
| 11 | E-22 | 6.9 ± 0.4 | 12.0 | 0.73 ± 0.57 | 0.082 ± 0.003 |
| 12 | E-32 | 7.1 ± 0.2 | 6.1 | 0.48 ± 0.17 | --- |
| 13 | B-08 | 33.0 ± 10.5 | 5.5 | 6.37 ± 3.68 | --- |
| 14 | E-13 | 30.3 ± 5.8 | 10.4 ± 5.8 | 1.20 ± 0.69 | 0.065 ± 0.002 |
| 15 | E-24 | 17.0 ± 3.4 | 8.9 ± 2.7 | 0.82 ± 0.32 | --- |
| 16 | E-45 | 14.8 ± 1.5 | 8.6 ± 2.4 | 0.52 ± 0.30 | --- |
| 17 | E-11 | 17.2 ± 2.1 | 11.6 ± 2.6 | 1.01 ± 0.48 | --- |
| 18 | D-08 | 29.9 ± 9.2 | 8.6 ± 2.0 | 16.8 ± 24.2 | 0.121 ± 0.002 |
| 19 | D-06 | 40.9 ± 9.6 | 11.4 ± 2.5 | 5.40 ± 3.20 | 0.056 ± 0.002 |
| 20 | C-14 | 19.9 ± 2.1 | 15.0 ± 5.0 | 4.57 ± 4.57 | --- |
| 21 | D-11 | 36.8 ± 12.6 | 10.6 ± 5.0 | 17.1 ± 10.2 | --- |
| 22 | D-10 | 18.0 ± 2.7 | 11.2 | 5.31 ± 2.76 | 0.264 ± 0.003 |
| 23 | E-25 | 25.3 ± 4.6 | 4.9 ± 1.0 | 1.89 ± 0.56 | --- |
| 24 | E-39 | 35.3 ± 12.3 | 9.1 ± 2.4 | 4.62 ± 2.81 | --- |
| 25 | E-16 | 35.1 ± 3.2 | 13.4 ± 14.4 | 2.84 ± 2.93 | --- |
| 26 | E-12 | 31.2 ± 9.5 | 12.5 ± 3.1 | 0.97 ± 0.73 | --- |
| Means avg.±s.d. | | 23.2 ± 10.6 | 13.4 ± 5.6 | 3.17 ± 4.47 | 0.142 ± 0.082 |
| S.D.'s avg.±s.d. | | 4.7 ± 3.7 | 4.4 ± 3.4 | 2.65 ± 4.94 | |

[a]Mean ± standard deviation of 4 measurements 1-2 m from the house on each of four sides.

[b]Single measurement and uncertainty based on gamma-ray counting statistics.

[c]Not measured.

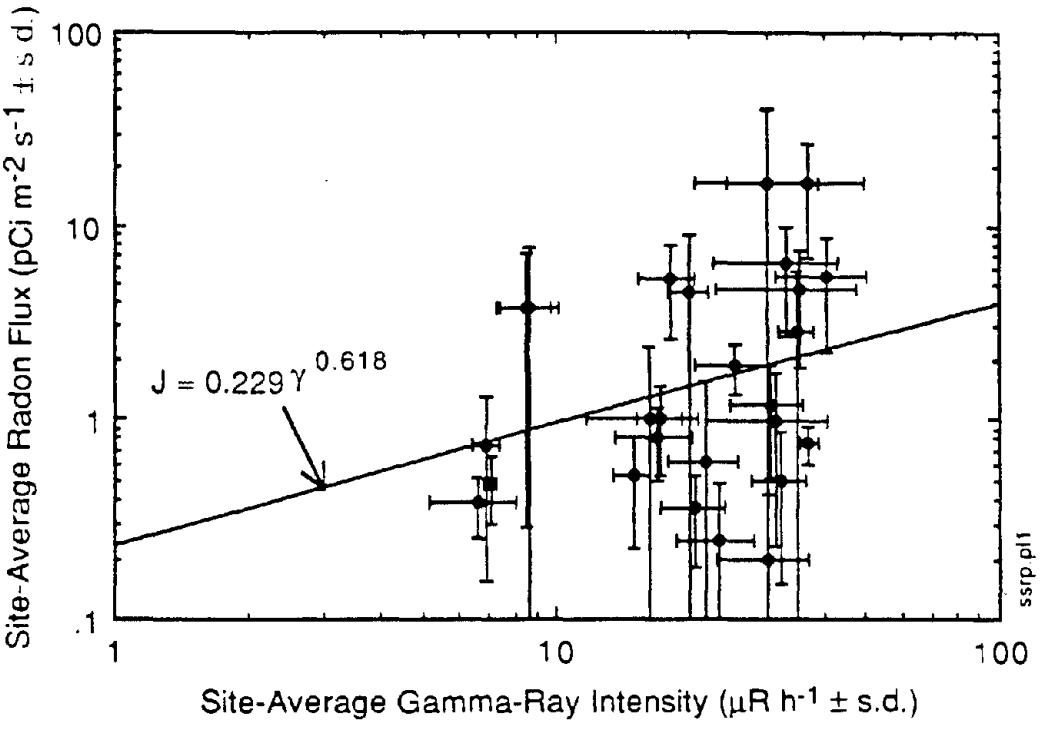


**Figure 3. Logarithmic regression of radon flux measurements on gamma-ray measurements for each site.**

Similar regressions of soil radon flux on soil moisture similarly exhibited a large amount of scatter, as may be expected because of the radium-dependence of radon flux in addition to its expected moisture dependence. The regression of soil radon flux on soil moisture exhibited a correlation coefficient of only r=0.26 for the fitted line $J_s = 6.9 - 0.268M_v$. Corresponding regressions of the site-averaged values, as reported in Table 4, yielded a slightly higher correlation coefficient of r=0.34 for the similar fitted line $J_s = 6.8 - 0.274M_v$. The data also were plotted logarithmically, as illustrated in Figure 4, and fitted to the line $J_s = 28\ M_v^{-1.18}$. Figure 4 illustrates the tendency for the low flux averages to be associated with high moisture levels.

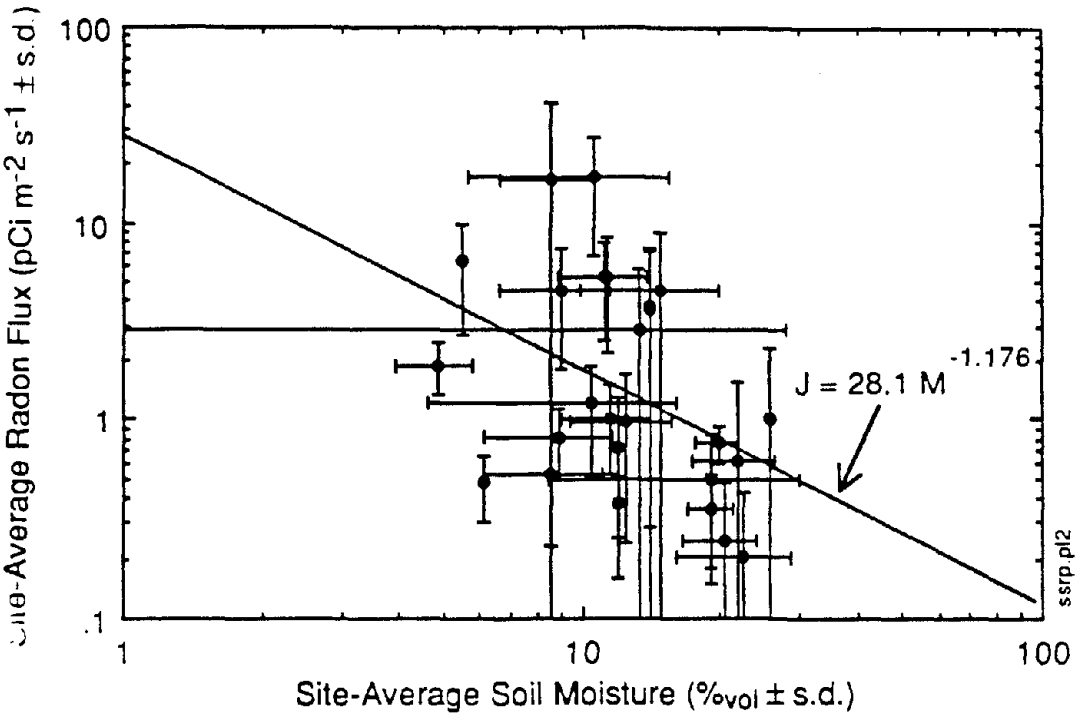


**Figure 4. Logarithmic regression of radon flux measurements on soil moisture for each site.**

The soil radon flux from a uniform soil profile is directly proportional to the soil radium concentration. It is also proportional to $\sqrt{D_s}\tanh(\alpha_s x_s)$, where $x_s$ is the thickness of the soil profile contributing to the flux (i.e., above the water table, and above bedrock). Therefore, the measured site radon fluxes also were regressed on the product of these parameters, which was defined as the surrogate flux parameter $J_{sur}$. The gamma-ray intensity was used as the surrogate for radium concentration, and S was calculated from site moisture data using equation (9) and the soil porosity in Table 2. The soil radon diffusion coefficient was calculated from the resulting value of S using equation (17). The regression of the measured soil radon fluxes on $J_{sur}$ had an improved correlation coefficient of r=0.55 for the fitted line $J_s = -0.85 + 1.51\ J_{sur}$. A logarithmic plot of this comparison is illustrated in Figure 5, with a least-squares fitted line corresponding to $J_s = 0.6\ J_{sur}$. Although this relation is a better predictor of radon flux than that depicted in Figure 3, it still exhibits considerable uncertainty, thus limiting its potential uses for predicting radon flux.

It should be noted that the radon flux measurements in Table 4 represent only a single point in time, and that measurements at other times or seasons may give a more representative estimate of annual-average conditions. The importance of temporal variation is demonstrated by a geometric standard deviation of nearly 2.1 in representing annual-average radon concentrations by a single charcoal canister measurement (Roe91). Thus, improved estimates of site radon potential could be obtained from measurements during different seasons. However, a prolonged measurement period would generally not satisfy the need for a rapid, one-time measurement of site radon potential.

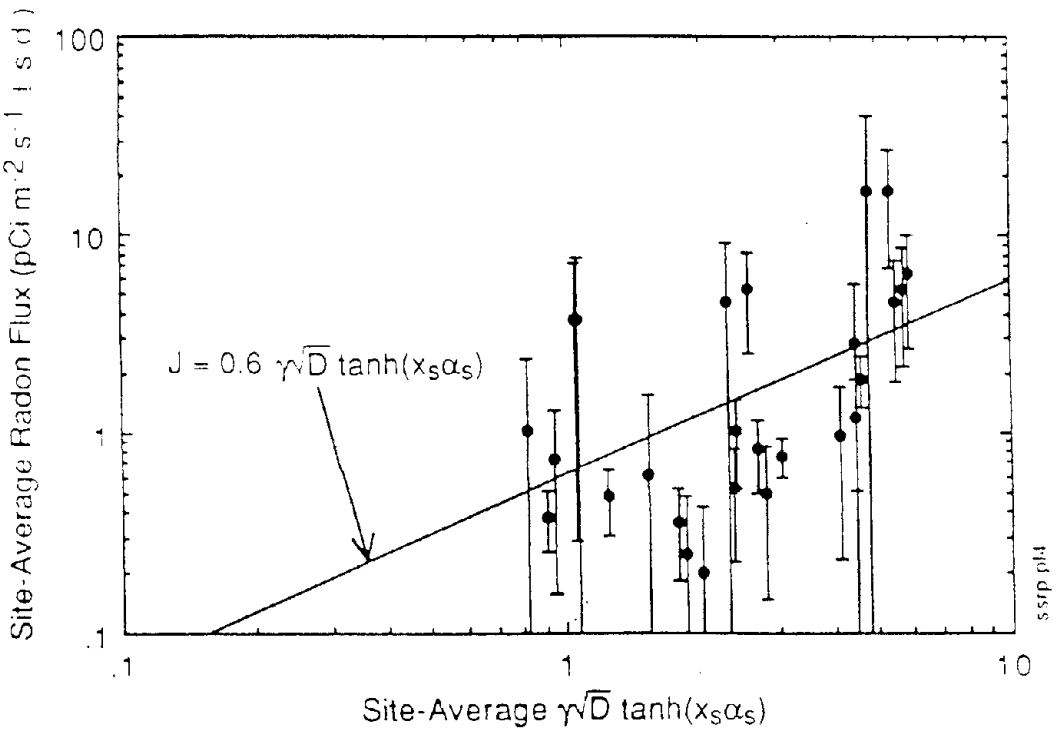


**Figure 5.** **Logarithmic regression of radon flux measurements on the surrogate flux parameter $J_{sur}$ for each site.**

## 4.2 ESTIMATION OF SITE-SPECIFIC SOIL RADON POTENTIALS

Site-specific soil radon potentials were estimated using equation (8). The soil water saturation fraction, S, was calculated from the measured volumetric moistures in Table 4 and a porosity of $\varepsilon$=0.407 from Table 2. $C_{sub}$ was calculated from the measured radon fluxes in Table 4 using equation (11). The calculated values follow the same trend, but are lower than the five measured values in Table 3. The lower values could result from drier soils beneath the slab (compared to yard-measured values), causing higher diffusion coefficients. The soil radon diffusion coefficient used in these calculations was obtained from equation (17), again using the same values for S and $\varepsilon$. Table 5 presents the resulting site-specific soil radon potentials, along with the calculated values of $C_{sub}$ and S. For comparison, Table 5 also presents the median soil radon potentials calculated from the draft FRRP soil radon potential map (Nie95a).

**Table 5. Comparison of site-specific and mapped soil radon potentials**

| RAE No. | FRRP No. | S (fraction) | $C_{sub}$ (pCi $L^{-1}$) | $Q_{ss}$ (mCi $y^{-1}$) | $Q_{map}$ (mCi $y^{-1}$) |
|---|---|---|---|---|---|
| 1 | E-34 | 0.54 | 795 | 1.47 | 5.91 |
| 2 | E-36 | 0.47 | 426 | 0.95 | 5.91 |
| 3 | E-30 | 0.47 | 591 | 1.33 | 5.91 |
| 4 | E-31 | 0.55 | 518 | 0.92 | 5.91 |
| 5 | E-42 | 0.49 | 911 | 1.95 | 2.48 |
| 6 | E-38 | 0.50 | 441 | 0.91 | 2.48 |
| 7 | E-35 | 0.63 | 1,560 | 2.16 | 2.48 |
| 8 | E-40 | 0.34 | 3,710 | 10.6 | 5.53 |
| 9 | E-41 | 0.34 | 3,730 | 10.7 | 5.53 |
| 10 | E-37 | 0.30 | 371 | 1.13 | 2.48 |
| 11 | E-22 | 0.30 | 699 | 2.12 | 2.48 |
| 12 | E-32 | 0.15 | 398 | 1.34 | 2.48 |
| 13 | B-08 | 0.14 | 5,080 | 17.3 | 6.92 |
| 14 | E-13 | 0.26 | 1,090 | 3.45 | 0.78 |
| 15 | E-24 | 0.22 | 726 | 2.35 | 0.78 |
| 16 | E-45 | 0.21 | 464 | 1.51 | 0.78 |
| 17 | E-11 | 0.28 | 948 | 2.91 | 0.78 |
| 18 | D-08 | 0.21 | 14,400 | 47.1 | 1.85 |
| 19 | D-06 | 0.28 | 5,010 | 15.4 | 1.85 |
| 20 | C-14 | 0.37 | 4,660 | 12.9 | 1.85 |
| 21 | D-11 | 0.26 | 15,500 | 48.6 | 1.85 |
| 22 | D-10 | 0.28 | 4,900 | 15.2 | 1.85 |
| 23 | E-25 | 0.12 | 1,490 | 5.10 | 0.78 |
| 24 | E-39 | 0.22 | 4,050 | 13.1 | 0.78 |
| 25 | E-16 | 0.33 | 2,780 | 8.12 | 0.78 |
| 26 | E-12 | 0.31 | 934 | 2.80 | 0.78 |

Using the neighborhood groupings listed in Table 3, the site-specific soil radon potentials from Table 5 were averaged for area-based comparisons with the mapped soil radon potentials. The averaging was done assuming log-normal distributions, consistent with previous statistics applied to the soil radon potential data (Nie95a). Figure 6 illustrates the resulting geometric means and geometric standard deviations with side-by-side comparisons with the median mapped soil radon potentials. For illustration purposes, the average of the seven neighborhood geometric standard deviations in $Q_{ss}$ was applied to the three houses not

associated with other houses in this study. As illustrated, the $Q_{ss}$ values were higher than the mapped radon potentials ($Q_{map}$) in six of the ten comparisons. In statistical analyses of the seven comparisons involving multiple houses, the $Q_{ss}$ values averaged 0.8 standard deviations higher than the $Q_{map}$ values. This average bias is not significant ($p<0.41$). However, the average absolute difference between the $Q_{ss}$ and $Q_{map}$ values was 1.9 standard deviations, which is significant at the $p<0.05$ level. The geometric mean of all 27 ratios of $Q_{ss}/Q_{map}$ was 2.02, with a geometric standard deviation of 4.7 (GSD of the mean is 1.35). The slight positive bias in $Q_{ss}$ may result in part from radon flux sampling near the houses, which generally causes a slight elevation in flux compared to an open-field sample that is not affected by a house foundation.

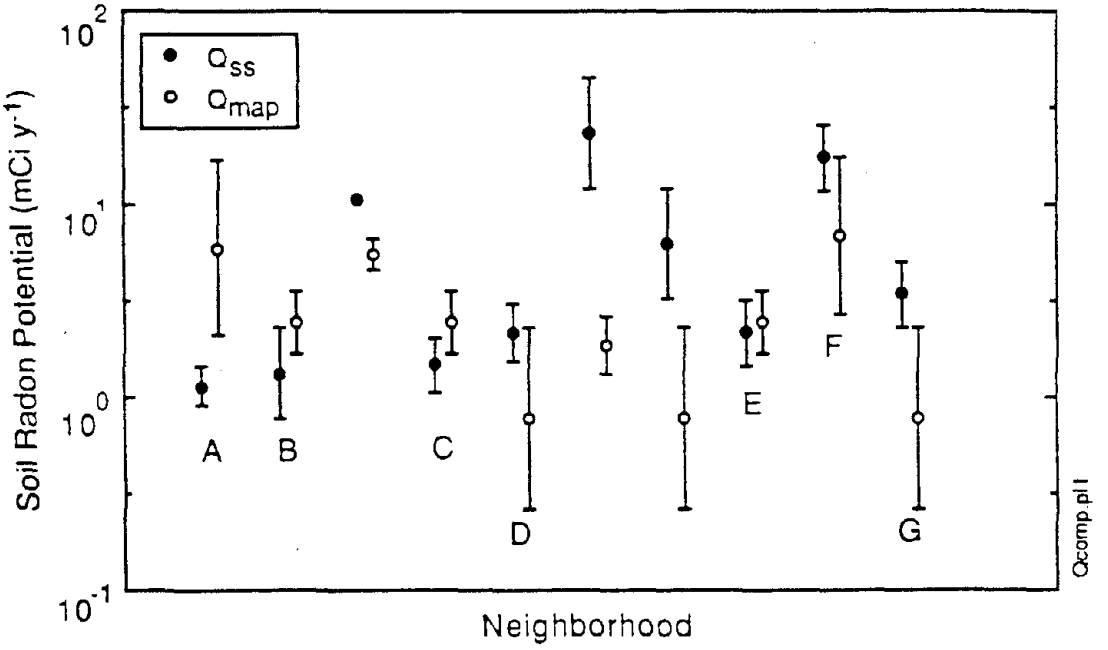


**Figure 6. Comparison of distributions of site-specific radon potentials calculated from measured data with radon potentials from the draft FRRP radon map (Nie95a).**

## 4.3 COMPARISON OF SOIL RADON POTENTIALS WITH INDOOR RADON DATA

Indoor radon concentrations were estimated from the soil radon potential measurements for comparison with the FRRP indoor radon data in Table 3. The indoor radon estimates utilized equations (6) and (7) to convert the measurements analyzed above for a reference house to represent the actual houses at the study sites. Three different calculations of indoor radon were performed. The first utilized the FRRP measured house ventilation data (Table 3); the second assumed a constant house ventilation rate of $\lambda_h$=0.25 air changes per hour (ach) for all of the houses; and the third was identical to the second except that it used the measured concrete-surface radon flux data as a direct estimator of $v_{slab}$.

Indoor radon concentrations were calculated using equations (6) and (7) with house-specific values of $V_h$, $A_h$, $C_{sub}$ (from Table 5), S (from Table 5), $x_h$, and $\lambda_h$ (extrapolated for 2.4 Pa pressure from values [Tys93] at higher pressures). Generic values of $v_{dc}$ and $v_{slab}$ were taken from the lumped-parameter model study (Nie94a). The resulting radon concentrations are presented in Table 6 for comparison with the measured indoor values. As indicated in Table 6, only one value was available for the slab-in-stem-wall houses (houses 1-13), but it was close to the measured value. The six comparisons for monolithic-slab houses (houses 14-26) averaged less than the measured values (0.53 ± 0.21), suggesting considerable uncertainty and bias in the model representation of the houses. The overall comparison for all seven houses was dominated by the monolithic-slab houses, with comparison ratios averaging 0.59 ± 0.24.

**Table 6. Comparison of measured and calculated indoor radon concentrations**

| RAE No. | FRRP No. | Meas'd Radon[a] (pCi $L^{-1}$) | Calculated with measured $\lambda_h$ | | Calculated assuming $\lambda_h$ = 0.25 ach | | Calculated using $J_{slab}$; $\lambda_h$=0.25 ach | |
|---|---|---|---|---|---|---|---|---|
| | | | (pCi $L^{-1}$) | calc./meas | (pCi $L^{-1}$) | calc./meas | (pCi $L^{-1}$) | calc./meas |
| 1 | E-34 | 2.1 ±0.1 | ---[b] | --- | 2.0 | 0.94 | 2.1 | 0.99 |
| 2 | E-36 | 1.9 ±0.4 | --- | --- | 1.3 | 0.73 | 2.0 | 1.09 |
| 3 | E-30 | 2.7 ±0.8 | --- | --- | 1.4 | 0.52 | 1.8 | 0.66 |
| 4 | E-31 | 1.6 ±0.4 | --- | --- | 0.8 | 0.52 | 1.1 | 0.68 |
| 5 | E-42 | 2.1 ±0.1 | --- | --- | 1.4 | 0.66 | 1.2 | 0.57 |
| 6 | E-38 | 2.2 ±0.8 | --- | --- | 1.2 | 0.55 | 1.0 | 0.45 |
| 7 | E-35 | 5.8 ±2.0 | --- | --- | 3.1 | 0.54 | 2.3 | 0.40 |
| 8 | E-40 | 4.4 ±0.6 | --- | --- | 6.6 | 1.52 | 5.7 | 1.31 |
| 9 | E-41 | 5.0 ±1.3 | --- | --- | 14.5 | 2.89 | 12.9 | 2.57 |
| 10 | E-37 | 1.9 ±0.4 | --- | --- | 1.7 | 0.90 | ---[c] | --- |
| 11 | E-22 | 3.0 ±0.4 | 2.8 | 0.93 | 3.0 | 0.98 | 2.8 | 0.94 |
| 12 | E-32 | 2.3 ±0.0 | --- | --- | 2.0 | 0.87 | --- | --- |
| 13 | B-08 | 37.5 | --- | --- | 23.3 | 0.62 | --- | --- |
| 14 | E-13 | 1.7 | 0.8 | 0.48 | 1.4 | 0.80 | 0.9 | 0.52 |
| 15 | E-24 | 2.0 | 0.7 | 0.35 | 0.9 | 0.46 | 0.4 | 0.22 |
| 16 | E-45 | 4.0 ±1.7 | --- | --- | 0.8 | 0.19 | --- | --- |
| 17 | E-11 | 1.6 ±1.1 | 0.8 | 0.48 | 1.2 | 0.75 | --- | --- |
| 18 | D-08 | 6.2 ±2.2 | --- | --- | 19.5 | 3.14 | 7.2 | 1.16 |
| 19 | D-06 | 3.0 ±0.5 | --- | --- | 6.8 | 2.26 | 2.6 | 0.87 |
| 20 | C-14 | 6.0 ±1.6 | --- | --- | 6.1 | 1.01 | --- | --- |
| 21 | D-11 | 14.8 ±3.6 | --- | --- | 20.6 | 1.40 | --- | --- |
| 22 | D-10 | 5.7 ±1.5 | --- | --- | 6.6 | 1.17 | 3.8 | 0.66 |
| 23 | E-25 | 2.4 ±0.6 | 1.9 | 0.79 | 1.9 | 0.79 | --- | --- |
| 24 | E-39 | 3.2 ±1.1 | --- | --- | 5.0 | 1.58 | --- | --- |
| 25 | E-16 | 2.5 ±0.8 | 1.9 | 0.78 | 3.1 | 1.26 | --- | --- |
| 26 | E-12 | 2.5 ±1.1 | 0.7 | 0.30 | 1.2 | 0.48 | --- | --- |
| SSW mean ± s.d.[d] | | | | 0.93 | | 0.94±0.65 | | 0.97±0.64 |
| Mono. mean ± s.d.[e] | | | | 0.53±0.21 | | 1.18±0.80 | | 0.69±0.35 |
| Total mean ± s.d. | | | | 0.59±0.24 | | 1.06±0.72 | | 0.87±0.56 |

[a]3-month alpha track measurement or mean ± standard deviation for two quarters.

[b]Dashes in this column indicate no data are available on house ventilation rates.

[c]Dashes in this column indicate radon flux was not measured from concrete surfaces.

[d]mean and standard deviation of ratios from slab-in-stem-wall houses.

[e]mean and standard deviation of ratios from monolithic-slab houses.

The second set of indoor radon concentrations were calculated as for the first set, but all house ventilation rates were defined from the default value $\lambda_h$=0.25 ach. This approach overcomes the limited data availability encountered with the first approach, and uses the ventilation rate defined for the reference house (Table 1). The results of these calculations also are presented in Table 6, and are again compared with the measured concentrations as calculated/measured radon ratios. As summarized at the bottom of Table 6, the 13 slab-in-stem-wall houses had ratios averaging 0.94 ± 0.65, and the monolithic-slab houses had ratios averaging 1.18 ± 0.80. The overall average ratio for all 26 houses was 1.06 ± 0.72. Despite the relatively large scatter, this set demonstrated much closer agreement of calculated and measured values, suggesting a possible bias in the earlier estimates of $\lambda_h$. A graphical comparison of the calculated and measured radon concentrations is shown in Figure 7a, where a wider range is illustrated for the calculated values than for the measured values. This can be partially explained by outdoor-air dominance of indoor radon levels at the low end of the measured range, since very low soil-related values will be dominated by airborne sources.

The third set of indoor radon concentrations was calculated as for the second set, using $\lambda_h$=0.25 ach, and also using the measured radon fluxes from concrete surfaces ($J_{slab}$). The concrete surface fluxes were divided by the sub-slab radon concentration to define more directly the value of $v_{slab}$. The results of these calculations also are presented in Table 6, and are again compared with the measured concentrations as calculated/measured radon ratios. As summarized at the bottom of Table 6, the slab-in-stem-wall houses had ratios averaging 0.97 ± 0.64, compared to 0.98 ± 0.74 for the corresponding ten houses by the previous approach. For Monolithic-slab houses, the ratio averaged 0.69 ± 0.35, compared to 1.57 ± 1.11 for the corresponding five houses by the previous approach. The overall average ratio for all 15 houses for which concrete surface fluxes were measured was 0.87 ± 0.56, compared to 1.18 ± 0.89 for the same houses by the previous approach. The consistently lower variation using the measured concrete fluxes shows that this measurement improves the estimate of radon transport through concrete over the generic assumption of equation (7). This approach demonstrates slightly larger biases, but involves significantly lower variations than the previous approach. Figure 7b graphically compares the calculated and measured radon concentrations, showing a trend similar to the previous set.

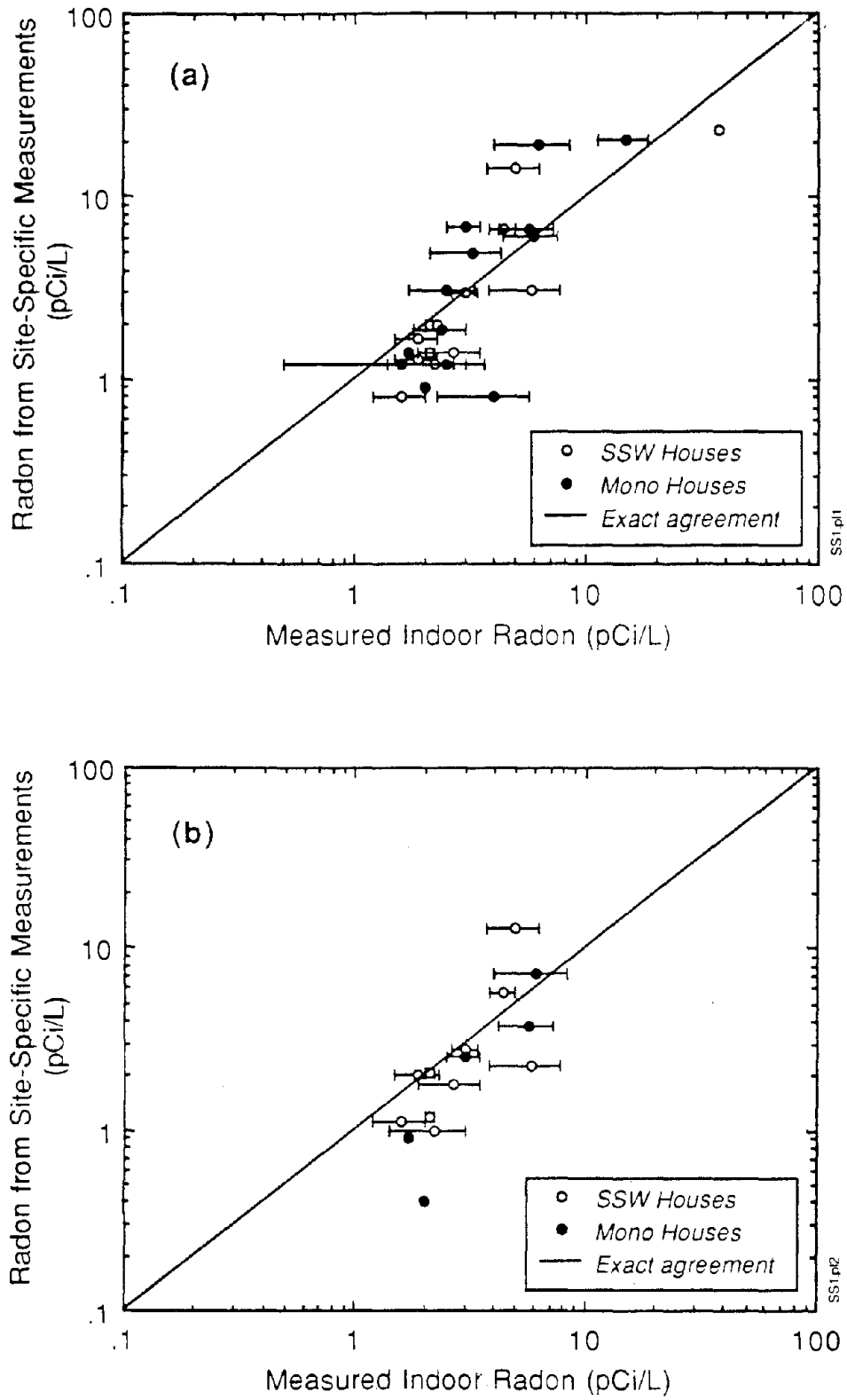


**Figure 7. Comparisons of indoor radon estimated from site-specific measurements with measured concentrations using (a) generic slab diffusion properties or (b) measured radon fluxes from concrete slabs.**

The comparisons of indoor radon data involve the differences of actual houses from the reference house in addition to uncertainty in radon potential measurement. The data in Table 6 demonstrate a 60-70% uncertainty in the ratios of calculated/measured radon ratios based on the site-specific radon potential measurements. In terms of geometric standard deviations, these variations correspond to a variation of GSD≈1.8. This is significantly less than the geometric standard deviation among the site-specific radon potential ratios, suggesting that the broad regional averaging required to generate radon potential maps introduces significant uncertainty when applied to specific individual sites. The lower variation in using the site-specific radon potential measurements also suggests the potential usefulness of such measurements. However, the geometric standard deviation of 1.8 among individual comparison ratios is far from ideal, particularly if the measurements are intended to determine the need for employing radon-resistant building features at a particular site.

# 5. DISCUSSION AND CONCLUSIONS

The analyses in this report demonstrate a theoretical basis for performing site-specific radon potential measurements using a variety of potential surrogate parameters. Although radon flux and soil moisture served in this report as the primary parameters for evaluation, other parameters, such as soil-gas radon concentration, soil air permeability, and others also are expected to provide useful results. The flux and moisture parameters used here were chosen because of previous analyses (Nie94a) that suggested a better correlation of radon potentials to soil radon flux than to soil-gas radon measurements. The present measurements also were chosen for their simplicity and relative cost-effectiveness.

Clearly, better precision and accuracy are expected if more detailed site characterization data are collected. For example, soil borings have occasionally been used to obtain detailed profiles of soil radium concentrations, radon emanation coefficients, and moisture levels, from which radon source and transport parameters were calculated (Nie94b). These data, along with improved house leakage measurements and radon monitoring, lead to data that support detailed numerical model analyses. With this more detailed (but more costly) approach, agreement between model results and empirical measurements has been demonstrated within 10-20%. Such model analyses can more accurately characterize site-specific soil radon potentials.

The present analyses suggest that unless a relatively detailed and expensive site characterization effort is conducted, simple site measurements may leave an uncertainty of nearly a factor of two (geometric standard deviation) in predicting indoor radon levels. Although this level of uncertainty may suffice for some purposes, it probably is inadequate for some decisions regarding construction of radon-resistant building features.

Planning and interpretation of site-specific radon potential measurements for building construction decisions should also consider the uncertainties in measurements and in achieving prescribed levels of radon resistance. If site-specific measurements are contemplated for reducing costs from "unnecessary" radon-resistant building features, an ample safety margin should be allowed for uncertainties in the measurements and in

predicting building performance. In some cases, effort spent in measuring the radon potential of a particular site may be better spent in conservatively including radon-resistant features in the building.

Risks associated with indoor radon should also be considered when deciding whether to include or avoid radon-resistant building features. In avoiding "unnecessary" building precautions, it is easy to falsely associate "safe" and "unsafe" levels with below 4 pCi $L^{-1}$ and above 4 pCi $L^{-1}$, respectively. The 4 pCi $L^{-1}$ level was chosen by the EPA only as a threshold for remedial action in existing houses, based on cost-benefit analyses (EPA92a). However, the EPA recommends further reduction of levels where possible to minimize residual health risks. For example, reduction of indoor radon from 4 pCi $L^{-1}$ to 2 pCi $L^{-1}$ lowers radon health risks by 50%, and further reductions are similarly proportional. Since radon-resistant features are generally less expensive in new construction than in remedial action, a cost-effective target threshold for new construction designs may be significantly lower than 4 pCi $L^{-1}$. Therefore, construction targeted at 4 pCi $L^{-1}$ from site-specific measurements could pose unnecessary risks to occupants if further building precautions could lower the indoor level inexpensively.

Both site-specific measurement costs and the EPA's estimated remedial action costs (EPA92a) should be considered in decisions concerning whether to implement radon-protective building features based on site-specific radon measurements. Appropriate safety margins are always needed to allow for uncertainties in measuring radon potentials, in constructing houses with prescribed radon resistances, and in measuring indoor radon levels. The safety margins give actual benefits of reduced health risk under EPA risk assessment methods, and therefore serve a greater purpose than simply assuring attainment of a $\leq$4 pCi $L^{-1}$ indoor radon goal.

## 6. LITERATURE REFERENCES


Acr90 Acres International Corp. Measurement of Crack and Opening Contribution to Radon Entry (Feasibility Study). Vol. III of Radon Entry Through Cracks in Slabs-on-Grade, Acres International Corp., report *PO9314*, 1990.

AST87 American Society for Testing and Materials, Standard Test Method for Determining Air Leakage Rate by Fan Pressurization, Philadelphia, PA: American Society for Testing and Materials, Designation *E779-87*, May 1987.

Cum92 Cummings, J.B., Tooley, J.J., and Moyer, N., Radon Pressure Differential Project, Phase I, FRRP, U.S. Environmental Protection Agency report *EPA-600/R-92-008* (NTIS PB92-148519), January 1992.

DSM85 DSMA Atcon, Ltd., A Computer Study of Soil Gas Movement into Buildings, Ottawa: Department of Health & Welfare, report *1389/1333*, 1985.

Eat84 Eaton, R.S. and Scott, A.G., Understanding Radon Transport into Houses, *Radiation Protection and Dosimetry* **7**: 251, 1984.

EPA89 Environmental Protection Agency, National Emission Standards for Hazardous Air Pollutants; Radionuclides; Final Rule and Notice of Reconsideration. Washington D.C.: U.S. Environmental Protection Agency, 40 CFR Part 61, *Federal Register* **54**:51654-51715, 1989.

EPA92a Environmental Protection Agency, Technical Support Document for the 1992 Citizen's Guide to Radon. Office of Radiation Programs, Washington D.C.: U.S. Environmental Protection Agency report *EPA-400-R-92-011*(NTIS PB 92-218395), May 1992.

EPA92b Environmental Protection Agency, A Citizen's Guide to Radon (Second Edition). Washington D.C.: U.S. Environmental Protection Agency, USDHHS, and USPHS report EPA-*402-K92-001*, May 1992.

EPA92c Environmental Protection Agency, National Residential Radon Survey Summary Report, Office of Air and Radiation, Washington D.C.: U.S. Environmental Protection Agency report EPA-402-R-92-011 (NTIS unassigned), October 1992.

Hin93 Hintenlang, D.E. and Al-Ahmady, K.K., Building Dynamics and HVAC System Effects on Radon Transport in Florida Houses. In Proceedings: The 1992 International Symposium on Radon and Radon Reduction Technology, Vol. 1, EPA-600/R-93-083a (NTIS PB93-196194), p. 6-93, May 1993.

Kun89 Kunz, C., Laymon, C.A., and Parker, C., Gravelly Soils and Indoor Radon. In Proceedings: The 1988 Symposium on Radon and Radon Reduction Technology, Vol. 1, *EPA-600/9-89/006a* (NTIS PB89-167480), p. 5-75, March 1989.

Naz87 Nazaroff, W.W., Lewis, S.R., Doyle, S.M., Moed, B.A., and Nero, A.V., Experiments on Pollutant Transport from Soil into Residential Basements by Pressure-Driven Airflow. *Environmental Science and Technology* **21**, 459-466, 1987.

Naz88 Nazaroff, W.W., Doyle, S.M., Nero, A.V., and Sextro, R.G., Radon Entry via Potable Water. pp. 131-157 in: *Radon and Its Decay Products in Indoor Air*, W.W. Nazaroff and A.V. Nero, eds., New York: Wiley & Sons, 1988.

Naz89 Nazaroff, W.W. and Sextro, R.G., Technique for Measuring the Indoor $^{222}Rn$ Source Potential of Soil, *Environmental Science and Technology* **23**, 451-458, 1989.

Nie91 Nielson, K.K. and Rogers, V.C., Feasibility and Approach for Mapping Radon Potentials in Florida, Research Triangle Park, NC: U.S. Environmental Protection Agency report *EPA-600/8-91-046* (NTIS PB91-217372), July 1991.

Nie92 Nielson, K.K. and Rogers, V.C., Radon Transport Properties of Soil Classes for Estimating Indoor Radon Entry. in: *Indoor Radon and Lung Cancer: Reality or Myth?*, F.T. Cross, ed., Richland, WA: Battelle Press, 357-372, 1992.

Nie93 Nielson, K.K., Protocol for Small-Canister Radon Flux Measurement, Salt Lake City, UT: Rogers & Associates Engineering Corp. protocol submitted to Florida Department of Community Affairs for inclusion in the FRRP Standard Measurement Protocols, May 1993.

Nie94a Nielson, K.K., Rogers, V.C., and Holt, R.B., Development of a Lumped-Parameter Model of Indoor Radon Concentrations, U.S. Environmental Protection Agency report *EPA-600/R-94-201* (NTIS PB95-142048), November 1994.

Nie94b Nielson, K.K., Rogers, V.C., Rogers, V., and Holt, R.B., The RAETRAD Model of Radon Generation and Transport from Soils into Slab-on-grade Houses, *Health Physics*, **67**, 363-377, 1994.

Nie95a Nielson, K.K., Holt, R.B., and Rogers, V.C., Statewide Mapping of Florida Soil Radon Potentials, Vol. 1, EPA-600/R-95-142a, September 1995.

Nie95b Nielson, K.K. and Rogers, V.C., Feasibility of Characterizing Concealed Openings in the House-Soil Interface for Modeling Radon Gas Entry, U.S. Environmental Protection Agency report *EPA-600/R-95-020 (NTIS PB95-178414)*, February 1995.

Pea90 Peake, R.T. and Schumann, R.R., Regional Radon Characterizations, in Field Studies of Radon in Natural Rocks, Soils, Land and Water, U.S. Geological Survey Bulletin, L.C.S. Gundersen and R.B. Wanty, eds., 1990.

Roe91 Roessler, C.E., Revell, J.W., and Wen, M.J., Temporal Patterns of Indoor Radon in North Central Florida and Comparison of Short-Term Monitoring to Long-Term Averages. In Proceedings: The 1990 International Symposium on Radon and Radon Reduction Technology, EPA-600/9-91-026a (NTIS PB91-234443), p. 3-131, July 1991.

Rog84a Rogers, V.C. and Nielson, K.K., Radon Attenuation Handbook for Uranium Mill Tailings Cover Design, Washington D.C.: U.S. Nuclear Regulatory Commission, *NUREG/CR-3533*, 1984.

Rog84b Rogers, V.C., Nielson, K.K., Sandquist, G.M., and Rich, D.C., Radon Flux Measurement and Computational Methodologies, Albuquerque, NM: U.S. Department of Energy report *UMTRA-DOE/AL-2700-201*, 1984.

Rog91a Rogers, V.C. and Nielson, K.K., Multiphase Radon Generation and Transport in Porous Materials, *Health Physics* **60**, 807-815, 1991.

Rog91b Rogers, V.C. and Nielson, K.K., Correlations for Predicting Air Permeabilities and $^{222}Rn$ Diffusion Coefficients of Soils, *Health Physics* **61**, 225-230, 1991.

Rog91c Rogers, V.C. and Nielson, K.K., Benchmark and Application of the RAETRAD Model. In Proceedings: The 1990 International Symposium on Radon and Radon Reduction Technology, Vol. 2, EPA/600-9-91-026b (NTIS PB91-234450), p. 6-1, July 1991.

Rog93 Rogers, V.C. and Nielson, K.K., Generalized Source Term for the Multiphase Radon Transport Equation, *Health Physics* **64**, 324-326, 1993.

Rog94 Rogers, V.C., Nielson, K.K., Lehto, M.A., and Holt, R.B., Radon Generation and Transport Through Concrete Foundations, U.S. Environmental Protection Agency report EPA-600/R-94-175 (NTIS PB95-101218), September 1994.

San91 Sanchez, D.C., Dixon, R. and Madani, M., The Florida Radon Research Program: Technical Support for the Development of Radon Resistant Construction Standards. In: The 1991 Annual AARST National Fall Conference Preprints, Vol. 1, p. 77-86, 1991.

Tan89 Tanner, A.B., A Tentative Protocol for Measurement of Radon Availability from the Ground. In Proceedings: The 1988 Symposium on Radon and Radon Reduction Technology, Vol. 2, *EPA-600/9-89-006b* (NTIS PB89-167498), p. 3-15, March 1989.

Tys93 Tyson, J.L. and Withers, C.R., Demonstration of Radon Resistant Construction Techniques, Phase II, EPA-600/R-95-159, November 1995.

Yok92 Yokel, F.Y. and Tanner, A.B., Site Exploration for Radon Source Potential, Gaithersburg, MD: U.S. Department of Commerce, National Institute of Standards and Technology report *NISTIR-5135*, 1992.